Journal of Imaging Science and Technology® 54(4): 040302–040302-6, 2010.

Deep Ultraviolet Radiation Simulates the Turin Shroud Image

Paolo Di Lazzaro, Daniele Murra and Antonino Santoni
ENEA, Department of Physical Technologies and New Materials, Frascati Research Center, via E. Fermi 45, 00044 Frascati, Italy
E-mail: paolo.dilazzaro@enea.it

Giulio Fanti
Department of Mechanical Engineering, University of Padua, via Venezia 1, 35131 Padua, Italy

Enrico Nichelatti
ENEA, Department of Physical Technologies and New Materials, Casaccia Research Center, via Anguillarese 301, 00123 Rome, Italy

Giuseppe Baldacchini
via Quattrucci 246, 00046 Grottaferrata, Italy

Abstract. *The faint yellowed body image embedded into the linen cloth of the Turin Shroud has peculiar chemical and physical characteristics that at the moment cannot be replicated all together in laboratory. The authors present experimental results of ArF excimer laser irradiation (wavelength 193 nm) of a raw linen fabric, seeking for coloration similar to that of the Shroud image. The authors achieved a permanent yellow coloration of linen as a threshold effect of the laser beam intensity and number of shots. Most important, the authors have achieved for the first time a submicrometer depth of coloration of the outermost part of the fibers, leaving a colorless fiber medulla. The authors also obtained latent coloration that appears after artificial aging of linen following laser irradiations that at first did not generate any visible effect. The authors have recognized different physical and chemical processes involved in both coloration and latent coloration. The comparison of the Turin Shroud image with the results of our ArF laser irradiation shows an interesting overlap of the main physical and chemical features.* © *2010 Society for Imaging Science and Technology.*
[DOI: 10.2352/J.ImagingSci.Technol.2010.54.4.040302]

INTRODUCTION

The Turin Shroud is a single piece of linen cloth measuring about 4.4 m by 1.1 m. Faint frontal and dorsal images of an apparently crucified man are embedded into the Shroud. These yellowish body images have peculiar chemical and physical characteristics[1] that have stimulated a worldwide scientific debate.[2–19]

Most of the scientific data on the Shroud image are from the work carried out by a team of 26 scientists under the auspices of the Shroud of Turin Research Project, Inc., (STURP) (1978), that performed an in-depth examination on the Shroud with electromagnetic energy, from infrared to x-rays, obtaining data leading to the analysis of the substances making up the body image and bloodstains.[4–12] The STURP measurements show that the body image is not painted, printed, singed by a heated bas-relief, or rubbed on a sculpture; moreover, the image color resides on the topmost fibers in the cloth weave. Reference 1 listed more than forty chemical and physical features of the Shroud image, and up to date all attempts to reproduce an image with the same microscopic and macroscopic aspect as well as all the chemical and physical characteristics have been unsuccessful. In this respect, the origin of the body image is still unknown.

This worldwide interest declined after the results of radiocarbon tests that placed the origins of the Shroud in the range 1260–1390 C.E.[20] However, recent results suggest the sample used for radiocarbon dating was not representative of the whole Shroud.[21,22] Independently of the controversial results of the radiocarbon test, a main concern is the origin of the body image on the Shroud, and this article addresses the search of a possible mechanism of the image formation.

Following the hints of independent works[14–19] showing that a burst of electromagnetic energy may account for the main image characteristics, we have considered the ultraviolet (UV) radiation as one of the best candidate for obtaining two of the main characteristics of the Shroud image, namely, a thin coloration depth and a low-temperature image-formation process.[1,11] Then, we used XeCl excimer laser radiation (wavelength 308 nm) to color linen by a sequence of UV laser pulses corresponding to a hypothetical burst of energy correlated with the Shroud image.[23] We have obtained a permanent coloration of linens that matches some characteristics of the Shroud images (appearance in cross-polarized light, fragility). However, the hue was too dark with respect to the Shroud images and the coloration thick-

Received Dec. 7, 2009; accepted for publication Jan. 26, 2010; published online Jun. 15, 2010.
1062-3701/2010/54(4)/040302/6/$20.00.

ness of linen yarns was too large compared to the topmost (approximately 0.2 μm thick) fiber coloration of the Shroud body image.[1,11,19]

In this article we present the results of linen irradiation using an ArF excimer laser emitting a deep UV wavelength $\lambda = 193$ nm significantly shorter than that emitted by XeCl lasers. In this way we obtained a substantial reduction in the coloration depth down to the outermost part of the linen yarns and a better overlap with the features of the Shroud image, including the hue of color (yellow after 193 nm irradiation, brown after the 308 nm irradiation). Most important, we have locally achieved for the first time a submicrometer depth of coloration of the outermost part of the fibers, leaving a colorless fiber medulla. We also single out some physical and chemical processes possibly leading to the improved results.

The main characteristics of the linen that are relevant in the interaction with deep UV radiation are described below. The next section summarizes the experimental setup and the conditions to achieve linen coloration by ArF laser pulses. We then analyze the irradiation results, and offer concluding remarks that summarize the main results.

OPTICAL CHARACTERISTICS OF LINEN

Linen fibers spun to produce linen yarns from which Shroud was woven are basically made of cellulose and hemicellulose.[24,25] The yellow-sepia Shroud image is superficial as it is located on the surface of the uppermost fibers, and the inside of these image-fibers does not show coloration.[1,10,11,26] Coloration was formed by an unknown process that caused oxidation, dehydration, and conjugation of the polysaccharide structure of the linen fibers to yield carbonyl groups and conjugated alkenes as the chromophore, i.e., a kind of premature aging process of the linen where double bonds C=C ultimately lead to the coloration of the image fibers of the Turin Shroud.[9,10,26]

We irradiated a linen fabric recently manufactured according to the ancient technology. It has 15 yarns/cm, the diameter of each yarn is 300 μm, and the diameter of the single fiber is ranging between 15 and 25 μm.

We have measured the absolute optical reflectance $R(\lambda)$ of this linen fabric in the spectral range (190–600 nm) using a Perkin Elmer Lambda 950™ spectrophotometer equipped with an integrating sphere having a diameter of 15 cm and coated with Spectralon. The results are plotted in Figure 1, also showing the reflectance of the Turin Shroud measured by Gilbert in the framework of the STURP studies.[4] Note the overlap of the measured reflectance of our linen with Gilbert's data. In addition, we also measured the absolute transmittance $T(\lambda)$ of our linen to finally estimate the spectral absorption $A(\lambda) = [1 - T(\lambda) - R(\lambda)]$ as shown in Figure 2.

ARGON FLUORIDE LASER IRRADIATION OF LINEN

The LPX-100i ArF excimer laser pulses (0.08 J/pulse in a 12 ns full width at half maximum pulse duration, 1 Hz repetition rate) are directly impinged onto linen textile fixed on a

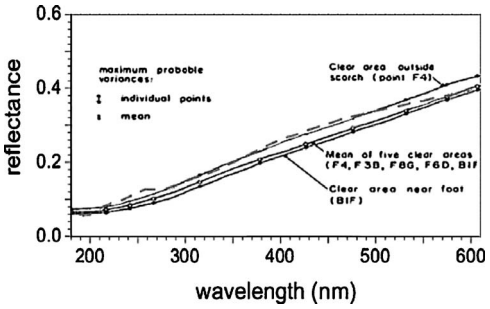

Figure 1. Dashed line: absolute spectral reflectance of our linen fabric measured using an integrating sphere having a diameter of 15 cm. Solid lines: absolute reflectance of the nonimage linen Shroud as reported in Ref. 4.

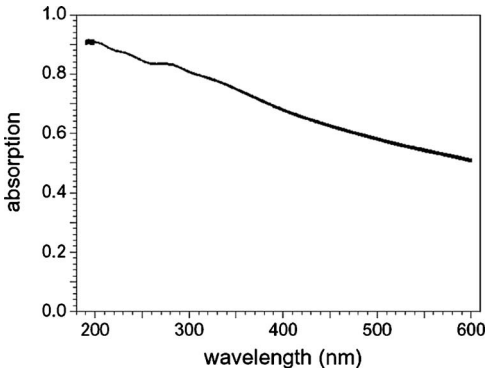

Figure 2. Spectral absorption of our linen estimated by the absolute spectral reflectance and transmittance measured on a Perkin Elmer Lambda 950™ equipped with an integrating sphere.

wooden frame; see Figure 3. Both energy and power densities on the linen are varied by moving it along the optical axis of the 1 m focal length lens that reduces the laser beam spot from the near-field size (3×1) cm^2 to a minimum size of (0.4×0.15) cm^2 obtained close to its focal plane. A fast photodiode connected with an oscilloscope TDS 520 monitors shot-to-shot fluctuations of both pulse-width and peak intensity of laser pulses.

We investigated a wide range of different combinations of laser intensity and number of shots. Table I reports a summary of some visual results on linen (observed under sunlight) as a function of the number of consecutive shots N, of the spatially averaged single-shot laser intensity I and fluence F, and of the total spatially averaged laser intensity I_T and fluence F_T, respectively, defined as

$$I = \frac{1}{A}\int\int_{\sigma} I(x,y)\,dx\,dy, \tag{1}$$

$$F = I \times \Delta t, \tag{2}$$

$$I_T = N \times I, \tag{3}$$

$$F_T = N \times F, \tag{4}$$

where A is the area of the laser spot, $I(x,y)$ is the local intensity value at the point with coordinates x,y within the

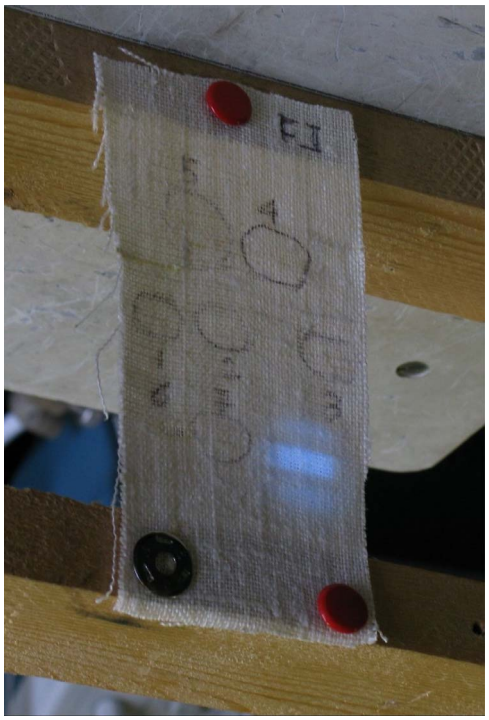

Figure 3. Blue fluorescence from the linen area just irradiated by a single ArF laser pulse.

irradiated spot σ, and Δt is the full width at half maximum of the laser pulse duration which was almost constant during irradiations.

Table I clearly shows that visually the results on linen are proportional to the total laser fluence and intensity. On the contrary, these results are not correlated with the single-shot intensity (fluence), cf., e.g., rows 1 and 2, and also compare the third row with the sixth, seventh, and eighth rows of Table I. A possible reason for this behavior is that even the single laser pulse modifies to some extent the linen surface so that each laser pulse interacts with a linen slightly modified by the previous laser shot. This cumulative effect becomes visible only when the total intensity and the total fluence are above the threshold values that are, respectively, $I_T > 1.8 \times 10^9$ W/cm^2 and $F_T > 22$ J/cm^2. In particular, a yellow coloration like that shown in Figure 4 is achieved when the combination of the single-shot intensity and fluence and the number of shots produces a total intensity and fluence in the range $I_T \approx (2-4) \times 10^9$ W/cm^2 and $F_T \approx (24-48)$ J/cm^2, respectively. When $I_T > 4.6 \times 10^9$ W/cm^2 ($F_T > 55$ J/cm^2) linen is ablated, and when $I_T > 6 \times 10^9$ W/cm^2 ($F_T > 72$ J/cm^2) a hole is burned.

The intensity and fluence values in Table I are "averaged" across the laser spot area. In fact, due to the imperfect uniformity of the laser beam profile, the local intensity value $I(x,y)$ will differ from the average intensity I. As a consequence, coloration was not uniformly distributed within the laser spot. In some cases we observed all the possible effects on linen within the same laser spot, as shown in Figure 5. That is, in the middle of the spot, where the local intensity is higher, we observed ablation of linen yarns, while one millimeter away, at an intermediate intensity level, yellowed yarns are clearly visible. At lower intensities, close to the spatial wings of the laser spot, linen yarns are unaltered. In this respect, the range of ArF laser parameters suitable to achieve a permanent coloration is even narrower than the range of XeCl laser parameters reported in Ref. 23.

ANALYSES

We observed fibers of linen placed between two crossed polarizers in a petrographic microscope to detect strains and defects in the crystalline structure of fibers induced by deep-UV radiation. The degree of birefringence of a linen fiber depends on its thickness, tensional status, and degree of racemization: thus a complex status of isochromatic areas results, depending on age, applied stress, presence of defects, and differing shapes of fibers. When fibers are aligned along the polarization axis of the analyzer, they are at extinction, and no birefringence is visible. When damage occurs in a given zone of the fiber aligned at extinction, it becomes birefringent and appears bright because the damaged zone has

Table I. Summary of the main results observed on linen as a function of the laser irradiation parameters. $I = (1/A) \times \int\int_\sigma I(x,y)dxdy$; $F = I \times \Delta t$; N = number of laser shots; $I_T = (N/A) \times \int\int_\sigma I(x,y)dxdy$; $F_T = I_T \times \Delta t$; A = area of the laser spot; $I(x,y)$ = local intensity value at the point with coordinates x, y within the irradiated spot σ; Δt = full width at half maximum laser pulse duration.

F (J/cm^2/shot)	I (MW/cm^2/shot)	N	F_T (J/cm^2)	I_T (MW/cm^2)	Macroscopic results on linen
0.420	35	30	12.6	1050	Unchanged
0.168	14	100	16.8	1400	Small surface change observed at grazing incidence light
0.432	36	50	21.6	1800	Light yellow coloration
0.126	10.5	200	25.2	2100	Yellow coloration
0.134	11.2	200	26.9	2240	Yellow coloration
0.079	6.6	402	31.8	2645	Yellow-sepia coloration
0.072	6	600	43.2	3600	Yellow-sepia coloration
0.160	13.3	500	79.8	6650	Ablated and hole burned

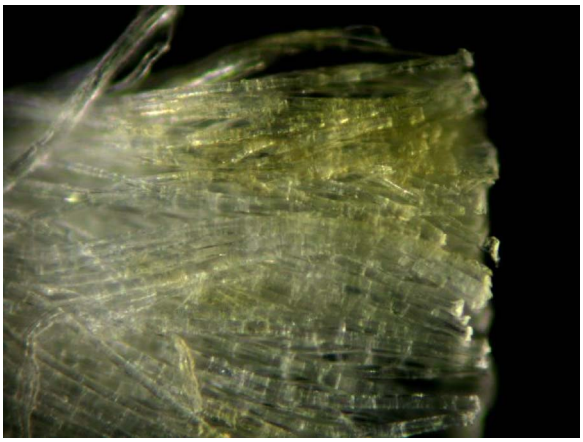

Figure 4. Microphotograph of a linen yarn irradiated with a total laser intensity $I_T = 2.2 \times 10^9$ W/cm^2 (corresponding to $F_T = 26$ J/cm^2). The yarn was opened by tweezers in order to improve visibility of the outermost colored fibers, as they are placed side by side with the noncolored ones.

Figure 5. Linen area irradiated by ArF laser pulses having different characteristics corresponding to the local laser intensity value $I(x,y)$. (1) Colored area. (2) Ablated area where fibers are first colored and then vaporized. (3) Area irradiated below threshold for coloration.

a different crystal orientation than the main part of the fiber. In our case, the irradiated parts of fibers displayed bright regions with fractures and defects, a behavior often observed in archeological linens.[10,11,27]

A suitable aging technique can color the irradiated area of linen even when no visible results are obtained by laser irradiation, as described in the following. We cut half of the laser spots on linen irradiated at $I_T = 1.4 \times 10^9$ W/cm^2 ($F_T = 16.8$ J/cm^2), i.e., below threshold for coloration (see Table I). One of the two parts was heated 10 s by an iron at the temperature of 190±10 °C, and a visible coloration of the heated part of the fabric appeared in the area corresponding to the laser spots, as shown in Figure 6. That is, the heating process, which simulates aging,[28] colored only the linen yarns irradiated just below threshold.

Moreover, when heating the laser spot on linen corresponding to the first row of Table I, no coloration appears. This allows us to fix the range for latent coloration as $I_T \approx (1.1-1.7) \times 10^9$ W/cm^2 corresponding to

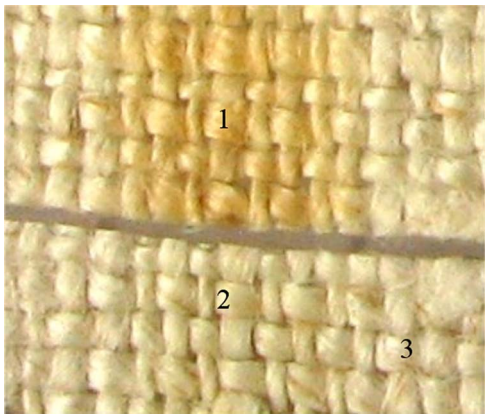

Figure 6. Linen fabric cut after a below-threshold irradiation. (1) Irradiated region after heating. (2) Irradiated region not heated. (3) Not irradiated region. Latent coloration of the linen area irradiated below threshold appears only after artificial aging of the upper part of irradiated linen.

$F_T \approx (13-20)$ J/cm^2. By the way, when heating a colored spot (i.e., one irradiated above the threshold for coloration) the yellow color becomes more visible as it shows a higher contrast with respect to surrounding unirradiated areas. The above latent image formation can be explained by cellulose oxidation and dehydration (responsible for the production of conjugated unsaturated structures) induced by heat. In fact, it is known that the coloring process of cellulose triggered by an initial exposure of UV light is accelerated and strengthened by heat.[28]

Concerning the depth of coloration, Figure 7 shows two linen yarns, respectively, irradiated by ArF and XeCl lasers. The difference is impressive, and microphotographs show that the color penetration depth in different linen yarns irradiated at ($\lambda = 193$ nm is 26±4 μm, a factor threefold to fivefold smaller than that achieved on irradiation at $\lambda = 308$ nm).

Most important, we found a few irradiated fibers showing a colorless medulla, see Figure 8, and it is likely that the coloration resides in the primary cell walls of these fibers, a property that closely resembles the very thin coloration depth of the image fibers of the Shroud.[1,10,11,26]

The different coloration depths shown in Fig. 7 are mainly due to the different wavelengths: in fact, the shorter λ allows a smaller penetration depth and thus a greater amount of energy absorbed for a unit volume. However, Fig. 2 shows only 11% difference in absorption between 193 and 308 nm. As a consequence, an additional mechanism is necessary to explain both the different depth of coloration and the different hue of color, namely, a yellow-sepia after 193 nm irradiation and a light-brown after 308 nm irradiation. This additional mechanism could be triggered by the spectral absorption peak below 260 nm of the ketonic carbonyls[29] that promote the formation of conjugated alkenes having C=C double bonds responsible for the yellowing. In other words, unlike 308 nm wavelength photons, deep UV, 193 nm photons are absorbed by ketonic carbonyls and bring about photolytic degradation of cellulose, causing

(a)

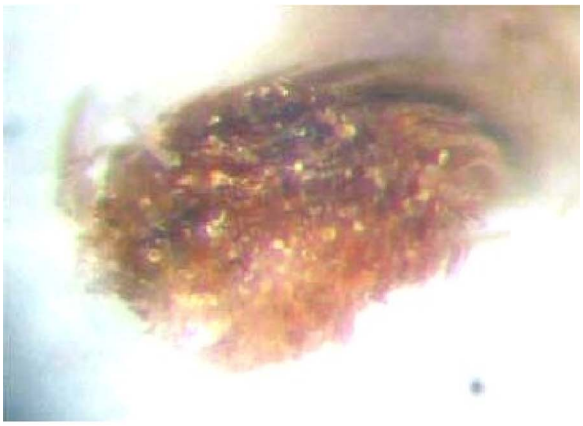

(b)

Figure 7. Cross section of two yarns of linen colored after irradiation with (a) (ArF laser ($\lambda = 193$ nm) and (b) XeCl laser ($\lambda = 308$ nm). After irradiation with ArF laser, (a) shows the color penetrates only the outermost fibers in the upper part of the yarn. Both yarns have an average diameter of 300 μm.

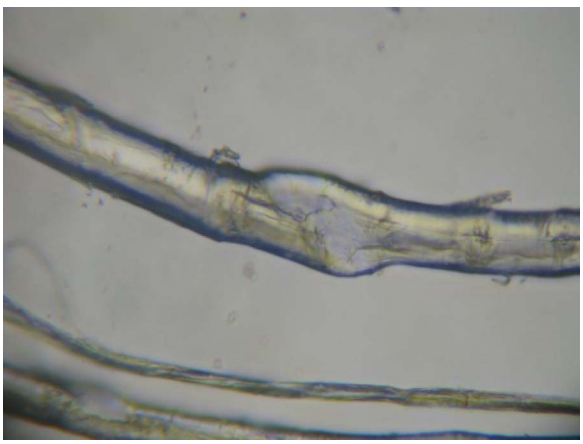

Figure 8. Image of a single linen fiber colored with ArF excimer laser pulses. The broken part in the middle shows a colorless inner medulla (tubular void in the centers of linen fibers).

molecular bond dissociation which promotes Shroud-like chromophoric changes.

Figure 9 shows the ultraviolet-fluorescence photograph of the irradiated linen. Note that, as in the case of the Shroud image fibers, the laser spot in the middle is not fluorescent under ultraviolet illumination. Figure 9 suggests that the laser spots quench or filter the fluorescence of the background linen.

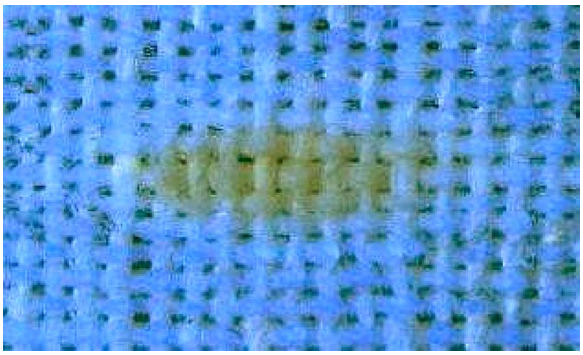

Figure 9. Ultraviolet induced fluorescence of a linen irradiated by ArF laser pulses at the working point of the third row of Table I. The irradiated area can be recognized by the lack of fluorescence.

CONCLUDING REMARKS

We have irradiated a linen fabric having the same absolute spectral reflectance of the Turin Shroud (see Fig. 1) with pulsed deep-UV radiation emitted by an ArF excimer laser. We have shown that 12 ns, 193 nm laser pulses are able to color a very thin layer on the linen yarn, as shown in Fig. 7(a). The colorless inner part of a few fibers like that shown in Fig. 8 suggests that we have locally achieved a coloration of the outermost part of the fibers. To the best of our knowledge, this is the first coloration of a linen material resembling the very shallow depth of coloration (0.2–0.5 μm) observed in the Turin Shroud fibers.[1,11,26]

The coloration is permanent, and we found a threshold effect in the spatially averaged total laser intensity I_T and fluence F_T, see Eqs. (3) and (4) and Table I. A yellowish coloration is achieved only in the range $I_T \approx (2-4) \times 10^9$ W/cm^2. Above this range linen is ablated, while a little below this range laser irradiations create latent images that appear only after artificial aging; see Fig. 6. When $I_T \leq 1.1 \times 10^9$ W/cm^2 linen is not colored at all.

Coloration can be only achieved over a very narrow range of laser parameters: even when I_T is above threshold for coloration, not all the irradiated fibers are colored; see Fig. 5. A comparison with previous results[23] shows that the shorter the wavelength, the smaller the color penetration depth (see Figs. 7 and 8) and the narrower the range of suitable laser parameters.

The hue of coloration depends on the laser wavelength and on the number of shots: linens irradiated at $\lambda = 308$ nm are light-brown colored,[23] while at $\lambda = 193$ nm photons induce a yellow coloration (see Fig. 4) similar to the color of the Shroud image. In both cases the image contrast increases with the number of laser shots. The different colors are probably due to different chemical reaction chains, respectively, triggered by the 308 nm and by the 193 nm radiation. In particular, the 193 nm radiation, thanks to the absorption of ketonic carbonyls[29] can induce a photolytic degradation of linen cellulose that promotes formation of

chromophores based on C=C double bonds that ultimately lead to the yellow coloration of the outermost part of the linen fibers.[9,26,29]

Some deep UV-induced defects in the crystalline structure of fibers observed by a petrographic microscope show analogies to those observed in image fibers of the Shroud.[27] The lack of UV-induced fluorescence observed in an irradiated spot (see Fig. 9) is an additional characteristic of our coloration that resembles the Shroud image.

In summary, our results demonstrate that a short and intense burst of directional deep-UV radiation can provide a linen coloration having many peculiar features of the Turin Shroud image, including hue, coloration of only the outermost fibers of the linen yarns, and lack of fluorescence.

REFERENCES

[1] G. Fanti, B. Schwortz, A. Accetta, J. A. Botella, B. J. Buenaobra, M. Carreira, F. Cheng, F. Crosilla, R. Dinegar, H. Felzmann, B. Haroldsen, P. Iacazio, F. Lattarulo, G. Novelli, J. Marino, A. Malantrucco, P. Maloney, D. Porter, B. Pozzetto, R. Schneider, N. Svensson, T. Wally, A.D. Whanger, and F. Zugibe, "Evidences for testing hypotheses about the body image formation of the Turin Shroud", The Third Dallas International Conference on the Shroud of Turin, 2005 (unpublished) www.shroud.com/pdfs/doclist.pdf

[2] B. J. Culliton, "The mystery of the Shroud challenges 20th-century science", Science **201**, 235–239 (1978).

[3] J. Allday, "The Turin Shroud", Phys. Educ. **40**, 67–73 (2005).

[4] R. Gilbert and M. Gilbert, "Ultraviolet-visible reflectance and fluorescence spectra of the Shroud of Turin", Appl. Opt. **19**, 1930–1936 (1980).

[5] E. J. Jumper and W. Mottern, "Scientific investigation of the Shroud of Turin", Appl. Opt. **19**, 1909–1912 (1980).

[6] S. F. Pellicori, "Spectral properties of the Shroud of Turin", Appl. Opt. **19**, 1913–1920 (1980).

[7] J. S. Accetta and J. S. Baumgart, "Infrared reflectance spectroscopy and thermographic investigations of the Shroud of Turin", Appl. Opt. **19**, 1921–1929 (1980).

[8] R. A. Morris, L. A. Schwalbe, and J. R. London, "X-ray fluorescence investigation of the Shroud of Turin", X-Ray Spectrom. **9**, 40–47 (1980).

[9] J. H. Heller and A. D. Adler, "A chemical investigation of the Shroud of Turin", Can. Soc. Forens. Sci. J. **14**, 81–103 (1981).

[10] L. A. Schwalbe and R. N. Rogers, "Physics and chemistry of the Shroud of Turin: A summary of the 1978 investigations", Anal. Chim. Acta **135**, 3–49 (1982).

[11] R. N. Rogers and A. Arnoldi, "Scientific method applied to the Shroud of Turin: A review" www.shroud.com/pdfs/rogers2.pdf (2002).

[12] E. J. Jumper, A. D. Adler, J. P. Jackson, S. F. Pellicori, J. H. Heller, and J. R. Druzik, "A comprehensive examination of the various stains and images on the Shroud of Turin", *Archaeological Chemistry III: ACS Advances in Chemistry 205*, edited by J. B. Lambert (American Chemical Society, Washington, 1984), pp. 447–476.

[13] W. C. Mc Crone, "The Shroud image", Microscope **48**, 79–85 (2000).

[14] J. P. Jackson, E. J. Jumper, and W. R. Ercoline, "Correlation of image intensity on the Turin Shroud with the 3D structure of a human body shape", Appl. Opt. **23**, 2244–2270 (1984).

[15] J. P. Jackson, "Is the image on the Shroud due to a process heretofore unknown to modern science?", Shroud Spectrum International **34**, 3–29 (1990).

[16] G. Fanti and M. Moroni, "Comparison of luminance between face of Turin Shroud man and experimental results", J. Imaging Sci. Technol. **46**, 142–154 (2002).

[17] G. Fanti and R. Maggiolo, "The double superficiality of the frontal image of the Turin Shroud", J. Opt. A, Pure Appl. Opt. **6**, 491–503 (2004).

[18] G. Fanti, "Can a corona discharge explain the body image of the Turin Shroud?", J. Imaging Sci. Technol. **54**, 020508 (2010).

[19] G. Fanti and R. Basso, *The Turin Shroud: Optical Research in the Past, Present and Future* (Nova Science, New York, 2008).

[20] P. E. Damon, D. J. Donahue, B. H. Gore, A. L. Hatheway, A. J. T. Jull, T. W. Linick, P. J. Sercel, L. J. Toolin, C. R. Bronk, E. T. Hall, R. E. M. Hedges, R. Housley, I. A. Law, C. Perry, G. Bonani, S. Trumbore, W. Woelfli, J. C. Ambers, S. G. E. Bowman, M. N. Leese, and M. S. Tite, "Radiocarbon dating of the Shroud of Turin", Nature (London) **337**, 611–615 (1989).

[21] R. N. Rogers, "Studies on the radiocarbon sample from the Shroud of Turin", Thermochim. Acta **425**, 189–194 (2005).

[22] M. S. Benford and J. G. Marino, "Discrepancies in the radiocarbon dating area of the Turin Shroud", Chem. Today **26**, 4–10 (2008).

[23] G. Baldacchini, P. Di Lazzaro, D. Murra, and G. Fanti, "Coloring linens with excimer lasers to simulate the body image of the Turin Shroud", Appl. Opt. **47**, 1278–1285 (2008).

[24] S. Perez and K. Mazeau, "Conformation, structure and morphologies of cellulose", *Polysaccharides: Structural Diversity and Functional Versatility*, 2nd ed., edited by S. Dumitriu (M. Dekker Inc., New York, 2004), Chap. 2.

[25] Hemicellulose is a polysaccharide like cellulose, but it consists of shorter chains (500–3000 sugar units) as opposed to 7000–15,000 glucose molecules per polymer seen in cellulose.

[26] R. N. Rogers, "Cellulose decomposition and image formation", www.shroudstory.com/faq/turin-shroud-faq-08.htm (2004).

[27] R. N. Rogers, "The Shroud of Turin, radiation effects, aging and image formation", www.shroud.com/pdfs/rogers8.pdf (2005).

[28] M. Yatagai and S. H. Zeronian, "Effect of ultraviolet light and heat on the properties of cotton cellulose", Cellulose **1**, 205–214 (1994).

[29] A. Bos, "The UV spectra of cellulose and some model compounds", J. Appl. Polym. Sci. **16**, 2567–2576 (1972).